



Recent Advances in Micromechanics of Materials

Morphology and effective properties of multi-scale random sets: A review

Dominique Jeulin

Centre de morphologie mathématique, mathématiques et systèmes, Mines ParisTech, 35, rue Saint-Honoré, 77300 Fontainebleau, France

ARTICLE INFO

Article history:

Available online 29 March 2012

Keywords:

Mathematical morphology
 Multi-scale random sets
 Boolean model
 Homogenization
 RVE

ABSTRACT

Complex microstructures in materials often involve multi-scale heterogeneous textures, modeled by random sets derived from Mathematical Morphology. Our approach starts from 2D or 3D images; a complete morphological characterization by image analysis is performed, and used for the identification of a model of random structure. Morphological models enter into the prediction of effective properties by estimation, bounds, or from numerical simulations. Simulations of realistic microstructures are introduced in a numerical solver to compute appropriate fields (electric, elastic, ...) and to estimate the effective properties by numerical homogenization, accounting for scale dependent statistical fluctuations of the fields. Our approach is illustrated by various examples of multi-scale models: Boolean random sets based on Cox point processes and various random grains (spheres, cylinders), showing a very low percolation threshold, and therefore a high conductivity or high elastic moduli for a low volume fraction of a second phase. Multi-scale iterations of random media provide another source of morphologies with interesting overall properties.

© 2012 Académie des sciences. Published by Elsevier Masson SAS. All rights reserved.

1. Introduction

In the context of the analysis of the behavior of many materials, it is common to encounter a superposition of different scales, even in the continuum framework. For instance in nanocomposite materials, arrangement of aggregates (like carbon black) appears at different scales [1]. This multi-scale arrangement has implications on the prediction of the effective properties of such composites (like the conductivity, the dielectric permittivity or the elastic moduli), from the properties of the two components (charge and matrix), and their spatial distribution.

In this article, we introduce a general methodology for modeling these situations [2,3]. It is based on the theory of random sets [4–7]. The morphology is summarized and simulated by multi-scale random models accounting for the heterogeneous distribution of aggregates. Identification of the model is made from image analysis.

In the next sections, we develop the following points:

- Principle of random structure modeling;
- Models of multi-scale random sets, simulation of microstructures, and percolation;
- Change of scale in random media: multi-scale iterations of random media, and prediction of effective properties by numerical simulations.

2. Principle of random structure modeling

An appropriate way to deal with the heterogeneity of materials is to make use of a probabilistic approach, that enables us to generate realistic models and simulation of the microstructures.

E-mail address: dominique.jeulin@mines-paristech.fr.

When considering two-phase materials (for instance a set of particles A embedded in a matrix, the complementary set A^c), we use a model of random closed set (RACS) A [4–7], fully characterized from a probabilistic point of view by its Choquet capacity $T(K)$ defined on the compact sets K , from (1) below, where P denotes a probability:

$$T(K) = P(K \cap A \neq \emptyset) = 1 - Q(K) = 1 - P(K \subset A^c) \quad (1)$$

In practice, $T(K)$ can be estimated by area fraction measurements on 2D images, or from volume fraction estimation on 3D images (from true microstructures, or from simulations), after a morphological dilation of the set A by the set K [4–7], noted $A \oplus \check{K}$, where the symbol \oplus denotes the Minkowski addition ($A \oplus K = \bigcup_{x \in K} A_x$) and \check{K} is the symmetrical set of K with respect to the origin ($\check{K} = \{-x, x \in K\}$). It can alternatively be calculated in a closed form for a given theoretical model, as illustrated by all examples of random sets given in this paper. Eq. (1) is used for the identification of a model (estimation of its parameters, and test of its validity). Particular cases of morphological properties deduced from (1) are the volume fraction V_V (when the set K is made of a single point and the random set A is stationary), the covariance (a useful tool to detect the presence of scales or anisotropies, obtained when K is made of a pair of points), the distribution of distances r of a point in A^c to the boundary of A (when K is the ball of radius r). The access to 3D images of microstructures by means of X-ray microtomography [8] makes it possible to use 3D compact sets K (like balls $B(r)$ with various radii r) to characterize the random set.

3. One-scale models

The archetype of random structure model is a random point process. It represents the most simple kind of random structure, like small defects isolated in a matrix. As a particular case of RACS, a random point process is characterized by its Choquet capacity $T(K)$. For a locally finite point process, use can be made of the probability generating function $G_K(s)$ of the random variable $N(K)$ (random number of points of the process contained in K). We have, noting the mathematical expectation (or average) of a given quantity by $E\{\}$

$$G_K(s) = E\{s^{N(K)}\} = \sum_0^{\infty} P_n(K) s^n$$

where $P_n(K) = P\{N(K) = n\}$, P being a probability. From this definition, we have $1 - T(K) = G_K(0) = P\{N(K) = 0\}$. For example, a typical model is the Poisson point process. It is the prototype of random point process without any order, since the numbers of points of the process contained in any pair of sets without intersection are independent random variables. For the homogeneous Poisson point process (a stationary random closed set) with intensity θ (i.e. average number of points per unit volume in 3D), we have, $\mu(K)$ being the Lebesgue measure (volume in 3D) of the compact set K :

$$P_n(K) = \frac{(\theta \mu(K))^n}{n!} \exp(-\theta \mu(K)) \quad \text{and} \quad G_K(s) = \exp(\theta \mu(K)(s - 1))$$

This classical result is immediately derived from the stationarity of the process and from the independence of disjoint volumes.

Starting from a point process, more general models, called grain models, can be generated, like the Boolean model, multi-scale models from intersection of random sets, or the multi-scale Cox Boolean model.

3.1. Boolean model

Some materials (like porous media or composite materials) can be simulated by means of a basic random set model, namely by distributions of overlapping objects. A random set model, the Boolean model, was proposed by G. Matheron [4,5] to reproduce this situation. First, we consider a location of centers of grains by means of a Poisson point process with intensity θ . In this condition, a volume V contains a random number of centers N following a Poisson distribution with average value θV . Then a random set is obtained by the union of random grains (any compact set). For this model, the Choquet capacity is given by (2), where $\bar{V}(A' \oplus \check{K})$ is the average volume of the random primary grain A' , dilated by K :

$$T(K) = 1 - \exp -\theta \bar{V}(A' \oplus \check{K}) \quad (2)$$

As a particular case, the volume fraction V_V of the grains, is given by (3):

$$1 - V_V = q = 1 - \exp -\theta \bar{V}(A') \quad (3)$$

Using for K a pair of points, 3 points, or a ball with radius r gives access to the covariance, the third order moment, and to the spherical contact distribution (the distribution of the distance of a random point in A^c to the boundary of A). For a given population of random grains, these morphological functions are theoretically available from (2). In the special case of spherical grains, the distribution function of the spheres radii can be estimated from the covariance [9], and therefore the model can be identified from the two-point statistics, which is a one-dimensional information. In more general situations, the identification of the model requires higher order moments for estimating the population of random primary grains.

3.2. Percolation of the Boolean model

For materials made of components with a high contrast of properties, like for instance conducting carbon black in an insulating polymeric matrix, there is a strong effect on the macroscopic properties like the effective conductivity when a given phase percolates through the structure, inducing connected paths in the samples of the medium. Analytical estimations of the percolation of Boolean models of cylinders are available with the excluded volume model [10]. More recent analytical estimates of the percolation threshold of isotropic Boolean models with convex grains are based on the zeroes of the connectivity number [9,11,12]. They give an estimate of the percolation threshold p_c^1 of the grains and p_c^2 of A^c . These two percolation thresholds are different, as a result of the fact that the two sets A and A^c are non-symmetrical. It was shown in [12] that the critical intensities θ_c for which percolation is obtained can be evaluated as a function of the expectations of the integral of mean curvature $\bar{M}(A')$ and of the surface area $\bar{S}(A')$ of the random convex grain A' by the roots of the connectivity number:

$$\theta_c = \frac{1}{\pi^2 \bar{S}(A')^2} (48\bar{M}(A') \pm 8\sqrt{6}\sqrt{-\pi^3 \bar{S}(A') + 6\bar{M}(A')^2}) \tag{4}$$

The two percolation thresholds are estimated as a function of the expectation of the volume of the grain $\bar{V}(A')$ by (using the lower value of θ_c in (4) for p_c^1 , and the higher for p_c^2):

$$p_c^1 = 1 - \exp -\theta_c \bar{V}(A')$$

$$q_c = p_c^2 = \exp -\theta_c \bar{V}(A')$$

The percolation threshold can also be estimated on simulations of the microstructure. In many studied cases, the estimates given by (4) are close to the results of simulations made with a single type of grain. It appears that a Boolean model with anisotropic primary grains (for instance sphero-cylinders) shows a much lower percolation threshold (0.01145 for an aspect ratio $l/r = 100$ [10,13]) than for isotropic grains (0.2895 for spheres [14,15]). This happens even for a uniform distribution of orientations of the sphero-cylinders, giving an isotropic medium on the macroscopic scale. This can explain the expected outstanding mechanical, electrical or chemical properties of composites containing carbon nanotubes, mainly due to their shape, giving a low percolation threshold. The percolation of the complementary set of a Boolean model of spheres obtained analytically from the connectivity number and by simulations is given by 0.05698 and 0.0540 ± 0.005 respectively [13].

4. Models of multi-scale random sets

4.1. Combination of independent random sets to generate multi-scale random media

Starting from the basic models, more complex structures, such as superposition of scales, or fluctuations of the local volume fraction p of one phase can be generated in a simple way by a combination of various random sets, considering independent realizations. A convenient construction of multi-scale models makes use of the union or intersection of independent random sets A_i with different scales. In the case of intersections, $A = \bigcap_i A_i$, and it is easy to show that we have:

$$P(K) = P\left\{K \subset \left(\bigcap_i A_i\right)\right\} = \prod_i P\{K \subset A_i\} \tag{5}$$

The result (5) is exact without any approximation, whatever the independent random sets A_i and their scales. For instance the overall volume fraction is the product of the volume fractions of the A_i . Similarly the binary covariance $C(h) = P\{x \in A, x+h \in A\}$, and more generally the n -point probabilities are obtained as a product of the corresponding individual n -point probabilities. A lower bound of the corresponding percolation threshold p_c can be estimated by the products of percolation thresholds p_c^i when the scales are widely separated: $p_c \simeq \prod_i p_c^i$. This model was used to simulate the random distribution of carbon black in composites by means of the intersection of three Boolean models of spheres at different scales, reproducing the carbon black particles, aggregates, and zones of exclusion in the matrix [16]. The identification of the model is made from the measurement of the overall binary covariance on $C(h)$ images obtained by transmission electron microscope on thin sections of the material.

4.2. The multi-scale Cox Boolean model

Another way to account for a non-homogeneous distribution of random grains, is obtained by replacing the Poisson point process, to locate germs for random grains, by a Cox point process [17]. Consider a positive random function (RF) giving a non-homogeneous intensity $\theta(x)$. For any realization of this RF, a Poisson point process with intensity $\theta(x)$ is generated. For a given realization, the number of points in a domain D follows a Poisson distribution with average $\theta(D) = \int_D \theta(dx)$:

$$P_n(D) = P\{N(D) = n\} = \frac{\theta(D)^n}{n!} \exp(-\theta(D))$$

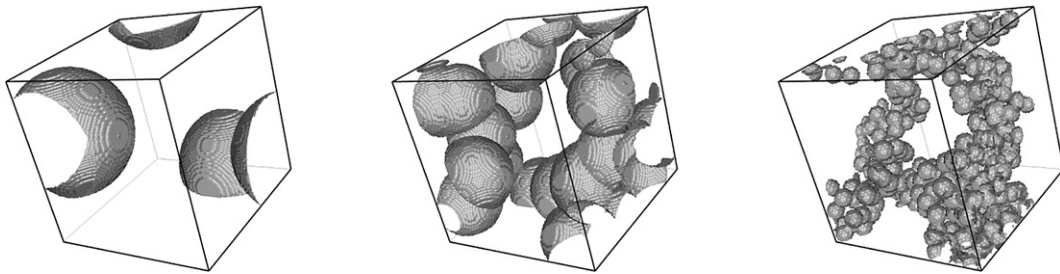


Fig. 1. Principle of 3D simulation of multi-scale random spheres aggregates. Left: exclusion spheres (distribution of radii $f_3(r)$), center: inclusion spheres ($f_2(r)$), right: aggregate spheres ($f_1(r)$).

Furthermore, for each realization, the number of points falling in any family of domains without any intersection are independent random variables. This is not anymore the case when considering the ensemble of realizations of the random intensity. If $\varphi_K(\lambda)$ is the Laplace transform with respect to the random function $\theta(x)$ of the positive random variable $E_{A'}\{\theta(A' \oplus \check{K})\}$, where $E_{A'}$ states for the mathematical expectation with respect to the random set A' , and E_θ the mathematical expectation with respect to the random function $\theta(x)$, we have:

$$T(K) = 1 - E_\theta\{\exp(-E_{A'}\{\theta(\check{A}' \oplus K)\})\} = 1 - \varphi_K(1) \quad (6)$$

An interesting particular case is obtained by means of a constant intensity θ inside a first random set A . For instance A is a Boolean model of spheres with a large radius R . In a second step we keep only the points of a Poisson point process contained in A , as germs for centers of spheres with a smaller radius r , so that there is no germ in the set A^c [14]. The random measure becomes $\theta(dx) = \theta 1_A(x) dx$, where $1_A(x)$ is the indicator function of the set A ($1_A(x) = 1$ if $x \in A$ and $1_A(x) = 0$ if $x \in A^c$). We have

$$T(K) = 1 - \Phi_K(\theta) \quad (7)$$

where $\Phi_K(\lambda)$ is the Laplace transform of the random variable $E_{A'}\{V((\check{A}' \oplus K) \cap A)\}$ obtained on the realizations of the random set A , after averaging over the realizations of the primary grain A' . As a particular case for a deterministic grain A' the Choquet capacity of the Boolean Cox model is deduced from the probability law of $V((\check{A}' \oplus K) \cap A)$. It is usually difficult to access to this law for any random set A , but it can be easily estimated from simulations. We can therefore estimate the theoretical covariance (or higher order moments) of the model.

In the case of a large separation of scales between the two sets A and A' we obtained an approximation of the $T(K)$ and then of $P(K)$ when assuming that $V(\check{A}' \oplus K) \rightarrow 0$ [3]. The covariance, the three-point probability and more generally any n -point probability and any moment $P\{K \subset A\}$ are asymptotically equal to the corresponding theoretical values (5) given for the intersection of independent random sets.

For carbon black nanocomposites, it is usual to model the distribution of carbon black particles by means of a three-scale model [16,14,1]: as illustrated in Fig. 1, spherical carbon particles (with a possible distribution of radii $f_1(r)$) are located on Poisson points inside inclusion zones (Boolean model of spheres with a distribution of radii $f_2(r)$) and outside of exclusion zones (Boolean model of spheres with a distribution of radii $f_3(r)$). The identification of the parameters of the model is made by means of an iterative optimization process, minimizing the difference between probabilistic properties of simulations and of images of the material: in [1], the multi-scale model is identified from measurements of the covariance, the third order moment, and of the area fraction after 2D closings on transmission electron images. To initialize the optimization process, use is made of the asymptotic approximation of the moments by the theoretical results obtained for independent random sets (5).

Another estimate of the Choquet capacity of the present version of the Cox Boolean model is obtained even for no large separation of scale. We consider a Boolean Cox random set built by considering implantations of a primary grain A' on the points of a Poisson point process with intensity θ inside a random set A . For a deterministic grain A' , with a good approximation the local volume fraction Z of the random set A inside $\check{A}' \oplus K$, $Z = V((\check{A}' \oplus K) \cap A) / V(\check{A}' \oplus K)$ follows a Beta distribution, with parameters α and β :

$$\begin{aligned} f(z) &= \frac{\Gamma(\alpha + \beta)}{\Gamma(\alpha)\Gamma(\beta)} z^{\alpha-1} (1-z)^{\beta-1} \\ E(Z) &= \frac{\alpha}{\alpha + \beta} \\ \text{Var}(Z) &= \frac{\alpha\beta}{(\alpha + \beta)^2(\alpha + \beta + 1)} \end{aligned} \quad (8)$$

The Laplace transform $\phi(\lambda)$ of the Beta distribution (8) is given by:

$$\phi(\lambda) = \frac{\Gamma(\alpha + \beta)}{\Gamma(\alpha)} \sum_{k=0}^{k=\infty} \frac{(-1)^k \lambda^k}{k!} \frac{\Gamma(\alpha + k)}{\Gamma(\alpha + \beta + k)} \tag{9}$$

and, using the property of the Γ function $\Gamma(\alpha) = (\alpha - 1)\Gamma(\alpha - 1)$

$$\frac{\Gamma(\alpha + \beta)}{\Gamma(\alpha)} \frac{\Gamma(\alpha + k)}{\Gamma(\alpha + \beta + k)} = \frac{(\alpha + k - 1) \cdots (\alpha + 1)\alpha}{(\alpha + \beta + k - 1) \cdots (\alpha + \beta)} \tag{10}$$

For a random set A with volume fraction p and with centered covariance $\bar{C}(h)$, we have

$$E(Z) = p \tag{11}$$

$$Var(Z) = \frac{1}{V(\check{A}' \oplus K)^2} \int_{\check{A}' \oplus K} \int_{\check{A}' \oplus K} \bar{C}(x - y) dx dy \tag{12}$$

For large volumes, when $V(\check{A}' \oplus K) \gg A_3$ (A_3 being the integral range deduced from the integral of the centered covariance of the random set A , as defined by Eq. (18) below), the variance becomes

$$Var(Z) = p(1 - p) \frac{A_3}{V(\check{A}' \oplus K)} \tag{13}$$

This can occur for sets $\check{A}' \oplus K$ that may not be considered as negligible with respect to A , while a large separation of scales was considered previously. The parameters α and β are expressed as a function of p and of $Var(Z)$ or of A_3 for large specimens, that are microstructural properties. We have:

$$\frac{\alpha}{\alpha + \beta} = p$$

$$\frac{\alpha\beta}{(\alpha + \beta)^2(\alpha + \beta + 1)} = \frac{\alpha}{\alpha + \beta} \frac{\beta}{\alpha + \beta} \frac{A_3}{V(\check{A}' \oplus K)}$$

and therefore

$$\alpha = p \left(\frac{V(\check{A}' \oplus K)}{A_3} - 1 \right) \tag{14}$$

$$\beta = (1 - p) \left(\frac{V(\check{A}' \oplus K)}{A_3} - 1 \right) \tag{15}$$

Similar expressions can be worked out for α and β from the expression (12), when the approximation (13) cannot be used, for instance for small volumes with $V(\check{A}' \oplus K) \lesssim A_3$. The Laplace transform $\Phi_K(\lambda)$ of the random variable $V((\check{A}' \oplus K) \cap A) = ZV(\check{A}' \oplus K)$, necessary to compute $T(K)$ from (7), is deduced from Eq. (9), replacing λ by $\lambda V(\check{A}' \oplus K)$, and using the values of α and β ((14) and (15)) in the expression (10). The Choquet capacity is then obtained from 7 by making $\lambda = \theta$. Variants of this model were developed for multi-scale fracture statistics models [3].

4.3. Percolation of the Cox Boolean model

As expected, the generation of aggregates produces random media with a lower percolation threshold: for a large separation of scales in a two-scale model, the lower bound of the overall percolation threshold p_c is given by the product $p_c^1 p_c^2$ of the corresponding thresholds, as in the case of the intersection of independent random sets. Models involving iteration of scales generate microstructure with a very low percolating threshold, and therefore with improved macroscopic properties when the percolating component presents the higher property (e.g. conductivity or elastic moduli). It shows that a typical homogeneous distribution of grains in space (like for the standard Boolean model) does not produce a medium with optimal properties for a given volume fraction. The percolation threshold of various multi-scale models was estimated in various situations [14,18,13]. In [13], we get $p_c = 0.0849$ for a scale factor equal to 30 in a two-scale Cox Boolean model of spheres, close to $0.2897^2 = 0.0839$. In [18] the percolation threshold of spherocylinders (aspect ratio $l/r = 100$) with centers located in a primary Boolean model of spheres (with $V_v = 0.32$) percolates for $p_c = 0.0056$. Again, considering the case of aggregates of carbon nanotubes, high performances are expected from such a microstructure for a very low volume fraction of charge, due to the presence of clusters of nanotubes.

5. Change of scale in random media

Studies of the effect of clustering of a second phase, like inclusions in a matrix, on the mechanical behavior of random composites were published in the recent years. It is not the scope of the present paper to make a systematic review of these studies. Some representative papers of different approaches are given by [19–22]. In [19], two-scale porous media with a perfectly plastic matrix are simulated for a comparison between a homogeneous distribution of voids and clusters of non-overlapping pores. The porosity is very low (less than 5%), and constant over 3D images of a low size (64^3 and 128^3), neglecting fluctuations of pore volume fraction. In [20], fluctuations of pore volume fraction at a mesoscale are accounted for in an analytical model of viscous material. Based on a Taylor expansion of the energy of the material with respect to the fluctuations of porosity, it is restricted to a weak variability of the pore volume fraction at a mesoscale. A weakening of the material with porosity fluctuations is predicted. The review on polymer nanocomposites [21] covers many topics, ranging from molecular dynamics to lattice gas models and mesoscale continuum models. The morphological models describing the mesoscale (pp. 222–232) are rather schematic and based on distributions of ellipsoidal particles with different orientations, or on phase separation patterns. These models are not in fact multi-scale in the same way as in our approach. Finally in [22], fluctuations of fiber volume fraction at a mesoscale are modeled and simulated by means of random functions, losing all information at the microscale. In these approaches, no construction of models of random set with multi-scale randomness is developed, and effects like the changes of physical behavior induced by the morphological percolation are ignored.

In what follows, the incidence of the presence of multiple scales in random media on their effective properties is illustrated by some examples.

5.1. Multi-scale iterations of random media

Using multi-scale iterations of random media gives processes to generate two-component microstructures with “optimal properties”, i.e. with the highest possible effective properties, given the volume fraction and the physical properties of components. The probably most famous case is given by the Hashin coated spheres assemblage [23]. It can be shown that for this isotropic morphology the effective conductivity (or effective dielectric permittivity) is given by the upper (resp. lower) Hashin–Shtrikman (H–S) bound when the material with the highest (resp. lowest) conductivity is put on the outer layer of spheres. We give here two other types of models, based on iterations of random sets.

5.2. Dilated Poisson hyperplanes

Third order bounds (depending on the three-point statistics of a random medium) of effective properties (like conductivity, elastic moduli) were derived in [24,25] from a classical variational principle. It was shown that for an isotropic two-component random set, these bounds depend on two positive functions of the parameters of the model of random set (like the volume fraction p among others), bounded by 1 [26]. When these functions summarizing the three-point probability of a random set are equal to 1 (resp. 0), the two third order bounds coincide with the upper (resp. lower) Hashin–Shtrikman (H–S) bound. We have shown [27,28] that for an infinite iteration of unions of dilated Poisson flats [29,30] (as illustrated in Fig. 2) with widely separated scales, we get a multi-scale structure percolating for any volume fraction, and corresponding to this situation: its effective permittivity is given by the upper (resp. lower) H–S bound, when attributing the highest permittivity to the union of dilated flats (resp. to their complementary set). This result is valid for a porous medium, where the upper (H–S) bound becomes the effective permittivity. The same result holds when considering the case of the bulk modulus κ in linear elasticity for well-ordered two-component media, satisfying $(\kappa_1 - \kappa_2)(\mu_1 - \mu_2) > 0$, μ being the shear modulus. Infinite-rank laminates studied in [31] provide another type of microstructure leading to the same optimal properties.

5.3. A two-scale hard-core composite

In some composites, a microstructure is made of non-overlapping objects (for instance spheres), described by a so-called hard-core process [6]. It turns out that for the sequential absorption version of this model generated with spheres of a single radius, numerical simulations show that the obtained effective properties are close to the lower H–S bound for a “soft” matrix, and close to the higher H–S bound for “soft” spheres (like pores) [32,33]. This was also observed on a microscopic scale, using 2D images (with dimensions $850 \mu\text{m}^2$) of a fiber composites larger than the RVE, the effective conductivity, bulk and shear moduli of images estimated by Finite Element computations being quite well predicted by the lower 2D H–S bound at that scale [34], so that fluctuations of effective properties between images can immediately be deduced from fluctuations of fiber area fraction at the scale of images of the microstructure. This proximity with the H–S bounds can be explained by the fact that for this model the morphological parameter involved in the calculation of bounds is close to 1 in the first case [35], and to 0 in the second one.

This point can be used to give an approximate estimate of the effective properties of a two-scale material containing non-overlapping aggregates (similar to the mentioned Cox Boolean model), obtained in two steps, as illustrated in an elastomeric matrix containing carbon black particles (CB) [1,33]. Composite spherical aggregates are made of percolating CB spheres (a Boolean model with volume fraction p_1) and of the elastomeric component (with volume fraction $1 - p_1$), as represented

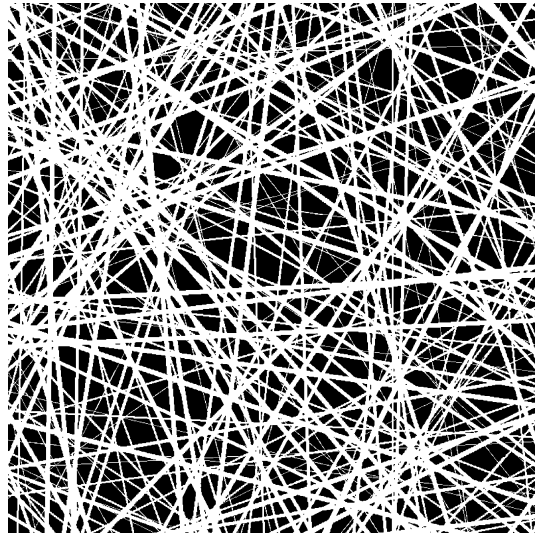


Fig. 2. 2D section of dilated Poisson planes.

in central and right parts of Fig. 1. The elastic properties of the aggregates are estimated by the third order upper bound of a Boolean model of spheres with volume fraction p_1 . In a second step, these spherical aggregates (with a radius much larger than the radius of CB spheres, involving a separation of scales) are implanted in the same elastomeric matrix according to a hard-core process forbidding overlaps between aggregates, with volume fraction p_2 , giving an overall volume fraction $p = p_1 p_2$. The overall moduli are now estimated by the H–S lower bound computed for this composite, and using the same matrix properties as before. As shown in [2], the estimates of the shear modulus G , obtained for different values of p_1 are consistent with the experimental measurements obtained for various mixes, a more uniform distribution in space giving a lower G . For a given CB volume fraction p , G increases when p_1 decreases, making easier the percolation in the two-scale model (the extreme value $p_1 = 1$ gives the standard hard-core two-component composite with moduli close to the lower H–S bound). A more accurate estimate is obtained by computer intensive numerical simulations [33], but the analytical model easily provides a good estimate of the elastic moduli.

5.4. Prediction of effective properties by numerical simulations

An efficient way to solve the problem of homogenization of physical properties, for instance to predict the dielectric permittivity or the effective mechanical properties of heterogeneous media, makes use of numerical solutions of the corresponding partial differential equations (PDE) solutions, before estimating the effective properties by spatial averaging of the solution. This requires the input of 3D images (real images, as obtained by confocal microscopy, or by X-ray microtomography) or simulations, so-called digital materials. In a second step a computational code (Finite Elements, Fast Fourier Transform FFT, PDE numerical solver) is implemented.

We extensively use a method based on the FFT, derived from [36,37], to estimate the equivalent macroscopic dielectric constant ε^* from the structure of a material and the properties of its constituents [38]. The numerical solution is obtained by means of the Green function of a homogeneous reference medium for the corresponding PDE for the electrical field or for the elastic field problem.

Using the FFT approach is very versatile and does not require any meshing of the microstructure, in contrast with other numerical methods such as Finite Elements. In elasticity, stress and strain field maps are obtained on the scale of microstructure, to get a detailed study of the effect of the microstructure on the local fields. With the Morph-Hom code developed by F. Willot [39,40] images of large sizes (up to 1600^3) can be handled for any contrast of properties, and therefore the electrostatic or elastic behavior of porous media or of rigid media could be successfully studied by numerical techniques. This was applied to the Boolean model of spheres with any volume fractions [39] and to two-scale and three-scale Cox Boolean models of spheres [40]. To check the validity of FFT calculations on multi-scale microstructures, several arguments were developed and illustrated in [40]. First, a comparison was made between the direct numerical simulations on 3-scale media and the iteration of calculations on 2-scale media after a first homogenization. The obtained effective properties coincide when the ratio of scales is of order of 10. A second control is made from the statistical approach of the RVE, summarized in the next section: the validity of Eqs. (17) and (19) have to be checked by plotting the change of the variance of fields with the volume of averaging subdomains (see for instance Fig. 11 in [40]). In addition, the integral range A_3 estimated from these plots should be much smaller than the smallest volume v involved in its estimation (typically $\frac{A_3}{v} \ll 10^3$ for 3D simulations), to insure the statistical representativeness of the simulations. We systematically apply this approach in our numerical studies.

The reinforcing effect of the iteration of scales with a large separation is clearly observed in the case of a very high conductivity or of a rigid phase, as a result of a lower percolation threshold. In the case of porous media, the reverse effect is observed, as would appear in the case of a damage at the interface between clusters of rigid particles and the matrix. A similar approach was applied to a microtomographic image of a mortar material [41]. A detailed study of the local enhancement of the stress field by the microstructure was made by means of image analysis of the maps obtained by FFT. From a quantitative study of the components of the 3D stress field at increasing distances from the boundaries of aggregates, a stress concentration was observed on a part of a surface defined by the 3D skeleton by zones of influence (SKIZ) of the aggregates. This is a promising approach to study the sensitivity of microstructural elements on damage, or to suggest new trial fields as input in variational principles.

5.5. Statistical approach of the RVE

When working on images of a material or on realizations of a random medium, a natural question arises [27,42]: what is the representativeness of the effective property estimated on a bounded domain of a microstructure? In other words, what is the size of a so-called “Representative Volume Element” RVE? In many industrial applications, mainly in the case of electronic parts such as MEMS, the size of the microstructure cannot be neglected with respect to the size of parts. The parts cannot be considered as an infinite homogeneous medium, as is almost always the case in standard homogenization of periodic or random media. On bounded domains, fluctuations of effective properties (often called apparent properties in the literature, while effective properties, independent on boundary conditions, are defined as limits for domains with an infinite extension) are observed and must be accounted for. We address this problem by means of a probabilistic approach giving size-dependent intervals of confidence, initially developed in the framework of the homogenization of the elastic moduli of random media [42,43], and based on the size effect of the variance of the effective properties of simulations of random media. This approach was applied to the elastic properties of rigid and of porous Boolean models of spheres [39,40], and to real materials like mortar [41] or fiber glass composites [34].

5.5.1. The integral range and scaling of the variance

We consider fluctuations of average values over different realizations of a random medium inside the domain B with the volume V . In Geostatistics [44], it is well known that for an ergodic stationary random function $Z(x)$, with mathematical expectation $E(Z)$, one can compute the variance $D_Z^2(V)$ of its average value $\bar{Z}(V)$ over the volume V as a function of the central covariance function $\bar{C}(h)$ of $Z(x)$ by:

$$D_Z^2(V) = \frac{1}{V^2} \int_B \int_B \bar{C}(x - y) dx dy \tag{16}$$

where

$$\bar{C}(h) = E\{(Z(x) - E(Z))(Z(x+h) - E(Z))\}$$

In Section 4.2 we were using the indicator function of the random set A , $Z(x) = 1_A(x)$. For a large specimen (with $V \gg A_3$), Eq. (16) can be expressed to the first order in $1/V$ as a function of the integral range in the space R^3 , A_3 , by

$$D_Z^2(V) = D_Z^2 \frac{A_3}{V} \tag{17}$$

$$\text{with } A_3 = \frac{1}{D_Z^2} \int_{R^3} \bar{C}(h) dh \tag{18}$$

where D_Z^2 is the point variance of $Z(x)$ (here estimated on simulations) and A_3 is the integral range of the random function $Z(x)$, defined when the integral in Eqs. (16) and (18) is finite. The asymptotic scaling law (17) is valid for an additive variable Z over the region of interest B . To estimate the effective elasticity or permittivity tensors from simulations, we have to compute the spatial average stress $\langle \sigma \rangle$ and strain $\langle \varepsilon \rangle$ (elastic case) or electric displacement $\langle D \rangle$ and electrical field $\langle E \rangle$. For the applied boundary conditions, the local modulus is obtained from the estimations of a scalar, namely the average in the domain B of the stress, strain, electric displacement, or electric field. Therefore the variance of the local apparent property follows Eq. (17) when the integral range A_3 of the relevant field is known. To be valid, the approach requires the stationarity and the ergodicity of the fields (σ or ε). This is satisfied for random media with stationary and ergodic moduli [28]. Since the theoretical covariance of the fields (σ or ε) is not available, the integral range can be estimated according to the procedure proposed by G. Matheron for any random function [45]: working with realizations of $Z(x)$ on domains B with an increasing volume V (or in the present case of homogenization, considering average values in subdomains v of large simulations, with a wide range of sizes), the parameter A_3 is estimated by fitting the obtained variance according to the expression (17). This parameter does not depend on V , provided it is large enough to insure the stationarity of the field by minimizing the effect of boundary conditions.

Some typical microstructures with long range correlations, like dilated Poisson hyperplanes mentioned in Section 5.2 or like dilated Poisson lines in 3D have an infinite integral range [29,30], so that the computation of the variance $D_Z^2(V)$ of Eq. (17) cannot be used anymore. In this situation, a scaling law by a power $\gamma < 1$ was suggested [46], and used in various applications where a coefficient close to 1 was empirically estimated [42,43]. With this scaling law, the variance becomes

$$D_Z^2(V) = D_Z^2 \left(\frac{A_3}{V} \right)^\gamma \quad (19)$$

where the volume A_3 is no more the integral of the central covariance function $\bar{C}(h)$, but is still homogeneous to a microstructural volume.

We have theoretically shown [47] that we have $\gamma = \frac{2}{3}$ for isotropic dilated Poisson lines in 3D, $\gamma = \frac{1}{3}$ for isotropic dilated Poisson hyperplanes in 3D (Fig. 2). When working in 2D, dilated Poisson lines can be used to model a fiber network [48]. In that case the variance of the area fraction scales with the inverse of the area of 2D images with an exponent equal to $\frac{1}{2}$. Therefore the decrease of the variance with the scale is much slower for these models as compared to situations with a finite integral range, like the Boolean model with compact primary grains. Simulations of the elastic properties and of the conductivity of 3D random fiber networks by finite elements [49] or by FFT [50] provide an empirical scaling law of the variance close to the theoretical one obtained for the volume fraction ($\frac{2}{3}$).

5.5.2. Practical determination of the size of the RVE

The size of an RVE can be defined for a physical property Z , a contrast, and a given precision in the estimation of the effective properties depending on the number n of realizations that are available. By means of a standard statistical approach, the absolute error ϵ_{abs} and the relative error ϵ_{rela} on the mean value obtained with n independent realizations of volume V are deduced from the 95% interval of confidence by:

$$\epsilon_{abs} = \frac{2D_Z(V)}{\sqrt{n}}; \quad \epsilon_{rela} = \frac{\epsilon_{abs}}{Z} = \frac{2D_Z(V)}{Z\sqrt{n}} \quad (20)$$

The size of the RVE can now be defined as the volume for which for instance $n = 1$ realization (as a result of an ergodicity assumption on the microstructure) is necessary to estimate the mean property Z with a relative error (for instance $\epsilon_{rela} = 1\%$), provided we know the variance $D_Z^2(V)$ from the asymptotic scaling law (17) or (19). Alternatively, we can decide to operate on smaller volumes (provided no bias is introduced by the edge effect resulting from the boundary conditions), and consider n realizations to obtain the same relative error. This methodology was applied to the case of the dielectric permittivity of various random media [51], and to the elastic properties and thermal conductivity of a Voronoï mosaic [42], of materials from food industry [52], or of Boolean models of spheres [39]. Further results were obtained for the Boolean model and for the multi-scale Cox Boolean model of rigid spheres (with radius 10 voxels, the larger scale being a Boolean model of spheres with radius 100 voxels). The results in [39] indicate that the largest RVE sizes for the one-scale model correspond to rigidly-reinforced media with $V_v \approx 0.49$. Accordingly, the variances $D_Z^2(V)$ and D_Z^2 , with $Z = \sigma_m$ (mean stress or 1/3 of the trace of the stress tensor), have been computed for the two-scale Cox Boolean model when $V_{v1} = V_{v2} = 0.7$ for a contrast higher than 10,000 of the bulk and shear moduli and a scale ratio equal to 10 [40]. It is found that the integral range of the two scales is increased by a factor close to 5.8 times, whereas the point variance increases by a factor 32. A 10% precision (i.e. $\epsilon_{rela} = 0.1$) is achieved when $V \approx 550^3$, which corresponds to an increase of the RVE by a factor $5.8 \times 32 = 5.7^3$. The drastic increase of the point variance in the case of the two-scale random medium underlies very large local stresses, that could induce more damage in the matrix if it contains defect, as compared to the one-scale model for the same volume fraction. Larger RVE, combined to the difficulty of observation of multi-scale microstructures in single images, make the experimental study of such materials much more challenging than their theoretical approach. However, in the case of a large separation of scales (for typically an order of magnitude as illustrated from simulations in [40]), investigations made at different resolutions are of common practice, and can be combined with iterative models, where the homogenization starts from the smaller scales.

The same approach was applied to a nonlinear behavior, namely for 2D/3D viscoplastic composite materials [53], the creep following a simple power law with exponents 3.5 in the hard phase and 4 in the soft phase. Shear tests were simulated under a macroscopic shear stress, and the statistical analysis was performed on the shear strain rate field. In that case it was found that for the same statistical precision, the linear elastic RVE was larger than the nonlinear RVE. The degree of generality of this result is not known. It is expected that in the case of a strong localization with a nonlinear behavior, long range correlations of the fields will appear, and scaling laws similar to the dilated Poisson hyperplanes (with a scaling exponent close to $\frac{1}{3}$) will be recovered, so that a slow convergence towards the effective properties could be observed on numerical simulations. This point remains to be investigated.

6. Conclusion

Multi-scale models of random media provide a wide variety of morphologies to simulate complex microstructures for application to real materials. These models are able to capture phenomena like the observation of very low percolation thresholds, explaining the enhancement of some effective properties for a low volume fraction of additions in a matrix.

Our approach is based on measurements obtained by image analysis, to test and select appropriate models, and to estimate their parameters. Combined to predictive models, by analytical means, or more generally by numerical simulations, the multi-scale models give access to the optimization of microstructures with respect to the required properties. This approach can be followed in many domains of application, like materials, nanocomposites, porous media, or biological media.

References

- [1] A. Jean, D. Jeulin, S. Forest, S. Cantournet, F. N'Guyen, A multiscale microstructure model of carbon black distribution in rubber, *Journal of Microscopy* 241 (3) (2011) 243–260.
- [2] D. Jeulin, Multi scale random models of complex microstructures, in: T. Chandra, N. Wanderka, W. Reimers, M. Ionescu (Eds.), *Thermec 2009, Materials Science Forum*, vols. 638–642, pp. 81–86.
- [3] D. Jeulin, Multi-scale random sets: from morphology to effective properties and to fracture statistics, in: *Proc. CMDS12, J. Phys.: Conf. Ser.* 319 (2011) 012013, doi:10.1088/1742-6596/319/1/012013.
- [4] G. Matheron, *Éléments pour une théorie des milieux poreux*, Masson, Paris, 1967.
- [5] G. Matheron, *Random Sets and Integral Geometry*, Wiley, New York, 1975.
- [6] J. Serra, *Image Analysis and Mathematical Morphology*, Academic Press, London, 1982.
- [7] D. Jeulin, Random texture models for materials structures, *Statistics and Computing* 10 (2000) 121–131.
- [8] E. Parra-Denis, C. Barat, D. Jeulin, Ch. Ducottet, 3D complex shape characterization by statistical analysis: Application to aluminium alloys, *Materials Characterization* 59 (2008) 338–343.
- [9] Th. Bretheau, D. Jeulin, Caractéristiques morphologiques des constituants et comportement élastique d'un matériau biphasé Fe/Ag, *Revue de Physique Appliquée* 24 (1989) 861–869.
- [10] I. Balberg, C.H. Anderson, S. Alexander, N. Wagner, Excluded volume and its relation to the onset of percolation, *Physical Review B* 30 (7) (1984) 3933–3943.
- [11] K. Mecke, D. Stoyan, The Boolean model: from Matheron till today, in: M. Bilodeau, F. Meyer, M. Schmitt (Eds.), *Space, Structure and Randomness*, in: *Lecture Notes in Statistics*, vol. 183, Springer-Verlag, Berlin, 2005, pp. 151–182.
- [12] D. Jeulin, Analysis and modeling of 3D microstructures, in: H. Talbot, L. Najman (Eds.), *Mathematical Morphology: From Theory to Applications*, ISTE/J. Wiley, New York, 2010 (Chapter 19).
- [13] D. Jeulin, M. Moreaud, Percolation d'agrégats multi-échelles de sphères et de fibres : Application aux nanocomposites, in: *Proc. Matériaux*, Dijon, 2006.
- [14] D. Jeulin, M. Moreaud, Multi-scale simulation of random spheres aggregates – Application to nanocomposites, in: J. Chraponski, J. Cwajna, L. Wojnar (Eds.), *Proc. 9th European Congress on Stereology and Image Analysis*, vol. 1, Zakopane, Poland, 2005, pp. 341–348.
- [15] M. Rintoul, S. Torquato, Precise determination of the critical threshold and exponents in a three-dimensional continuum percolation model, *Journal of Physics A: Mathematical and General* 30 (1997) L585–L592.
- [16] L. Savary, D. Jeulin, A. Thorel, Morphological analysis of carbon–polymer composite materials from thick sections, *Acta Stereologica* 18 (3) (1999) 297–303.
- [17] D. Jeulin, Modeling heterogeneous materials by random structures, Invited lecture, in: *European Workshop on Application of Statistics and Probabilities in Wood Mechanics*, Bordeaux, 22–23 March 1996, N-06/96/MM, Paris School of Mines Publication, 1996.
- [18] D. Jeulin, M. Moreaud, Percolation of multi-scale fiber aggregates, in: R. Lechnerova, I. Saxl, V. Benes (Eds.), *Proc. S4G, 6th Int. Conf. Stereology, Spatial Statistics and Stochastic Geometry*, Prague, 26–29 June 2006, Union Czech Mathematicians and Physicists, pp. 269–274.
- [19] N. Bilger, F. Auslender, M. Bornert, J.-C. Michel, H. Moulinec, P. Suquet, A. Zaoui, Effect of a nonuniform distribution of voids on the plastic response of voided materials: A computational and statistical analysis, *International Journal of Solids and Structures* 42 (2005) 517–538.
- [20] M. Gărăjeu, P. Suquet, On the influence of local fluctuations in volume fraction of constituents on the effective properties of nonlinear composites. Application to porous materials, *Journal of the Mechanics and Physics of Solids* 55 (2007) 842–878.
- [21] Q.H. Zeng, A.B. Yu, G.Q. Lu, Multiscale modeling and simulation of polymer nanocomposites, *Progress in Polymer Science* 33 (2008) 191–269.
- [22] J. Guillemainot, Ch. Soize, D. Kondo, Ch. Binetruy, Theoretical framework and experimental procedure for modelling mesoscopic volume fraction stochastic fluctuations in fiber reinforced composites, *International Journal of Solids and Structures* 45 (2008) 5567–5583.
- [23] Z. Hashin, The elastic moduli of heterogeneous materials, *Journal of Applied Mechanics* (1962) 143–150.
- [24] M.J. Beran, J. Molyneux, Use of classical variational principles to determine bounds for the effective bulk modulus in heterogeneous materials, *Quarterly of Applied Mathematics* 24 (1966) 107–118.
- [25] J. McCoy, On the displacement field in an elastic medium with random variations of material properties, in: *Recent Advances in Engineering Sciences*, vol. 5, Gordon and Breach, 1970, pp. 235–254.
- [26] G.W. Milton, Bounds on the elastic and transport properties of two-component composites, *Journal of the Mechanics and Physics of Solids* 30 (1982) 177–191.
- [27] D. Jeulin, Random structure models for homogenization and fracture statistics, in: D. Jeulin, M. Ostoj-Starzewski (Eds.), *Mechanics of Random and Multiscale Microstructures*, Springer-Verlag, Berlin, 2001, pp. 33–91.
- [28] D. Jeulin, Random structures in physics, in: M. Bilodeau, F. Meyer, M. Schmitt (Eds.), *Space, Structure and Randomness*, in: *Lecture Notes in Statistics*, vol. 183, Springer-Verlag, Berlin, 2005, pp. 183–222.
- [29] D. Jeulin, *Modèles morphologiques de structures aléatoires et de changement d'échelle*, Thèse de Doctorat d'Etatès Sciences Physiques, Université of Caen, 1991.
- [30] D. Jeulin, *Modèles de Fonctions Aléatoires multivariées*, *Sciences de la Terre* 30 (1991) 225–256.
- [31] G.W. Milton, Modeling the properties of composites by laminates, in: J.L. Ericksen, D. Kinderlehrer, R. Kohn, J.L. Lions (Eds.), *Homogenization and Effective Moduli of Materials and Media*, Springer-Verlag, Berlin, 1986, pp. 150–174.
- [32] J.C. Smith, The elastic constants of a particulate-filled glassy polymer: Comparison of experimental values with theoretical predictions, *J. Res. NBS* 80A (1976) 45–49.
- [33] A. Jean, F. Willot, S. Cantournet, S. Forest, D. Jeulin, Large scale computations of effective elastic properties of rubber with carbon black fillers, *International Journal of Multiscale Computational Engineering* 9 (3) (2011) 271–303.
- [34] M. Oumarou, D. Jeulin, J. Renard, Etude statistique multi-échelle du comportement élastique et thermique d'un composite thermoplastique, *Revue des composites et des matériaux avancés* 21 (2) (2011) 221–254.
- [35] S. Torquato, F. Lado, Effective properties of two-phase disordered composite media: II. Evaluation of bounds on the conductivity and bulk modulus of dispersions of impenetrable spheres, *Physical Review B* 33 (1986) 6428–6435.
- [36] D.J. Eyre, G.W. Milton, A fast numerical scheme for computing the response of composites using grid refinement, *European Physical Journal – Applied Physics* 6 (1999) 41–47.
- [37] H. Moulinec, P. Suquet, A numerical method for computing the overall response of nonlinear composites with complex microstructure, *Computer Methods in Applied Mechanics and Engineering* 157 (1998) 69–94.

- [38] S. Paciornik, O.F.M. Gomes, A. Delarue, S. Schamm, D. Jeulin, A. Thorel, Multi-scale analysis of the dielectric properties and structure of resin/carbon-black nanocomposites, *European Physical Journal – Applied Physics* 21 (2003) 17–26.
- [39] F. Willot, D. Jeulin, Elastic behavior of composites containing Boolean random sets of inhomogeneities, *International Journal of Engineering Sciences* 47 (2009) 313–324.
- [40] F. Willot, D. Jeulin, Elastic and electrical behavior of some random multiscale highly contrasted composites, *International Journal of Multiscale Computational Engineering* 9 (3) (2011) 305–326.
- [41] J. Escoda, F. Willot, D. Jeulin, J. Sanajuja, Ch. Toulemonde, Estimation of local stresses and elastic properties of a mortar sample by FFT computation of fields on a 3D image, *Cement and Concrete Research* 41 (2011) 542–556.
- [42] T. Kanit, S. Forest, I. Galliet, V. Mounoury, D. Jeulin, Determination of the size of the representative volume element for random composites: statistical and numerical approach, *International Journal of Solids and Structures* 40 (2003) 3647–3679.
- [43] G. Caillaud, D. Jeulin, Ph. Rolland, Size effect on elastic properties of random composites, *Engineering Computations* 11 (2) (1994) 99–110.
- [44] G. Matheron, *The Theory of Regionalized Variables and Its Applications*, Paris School of Mines, 1971.
- [45] G. Matheron, *Estimating and Choosing*, Springer-Verlag, Berlin, 1989.
- [46] Ch. Lantuejoul, Ergodicity and integral range, *Journal of Microscopy* 161 (1991) 387–403.
- [47] D. Jeulin, Variance scaling of Boolean varieties, Internal report N/10/11/MM, Paris School of Mines, 2011, hal-00618967, version 1.
- [48] Ch. Delisée, D. Jeulin, F. Michaud, Caractérisation morphologique et porosité en 3D de matériaux fibreux cellulosiques, *Comptes Rendus de l'Académie des Sciences, Série IIb* 329 (2001) 179–185.
- [49] J. Dirrenberger, S. Forest, D. Jeulin, M. Faessel, F. Willot, Modélisation de milieux fibreux aléatoires enchevêtrés et estimation de VER, Communication to Mecamat, Sophia Antipolis, 11 May 2011, in preparation.
- [50] H. Altendorf, 3D morphological analysis and modeling of random fiber networks, PhD thesis, Mines ParisTech, October 2011.
- [51] D. Jeulin, M. Moreaud, Volume élémentaire représentatif pour la permittivité diélectrique de milieux aléatoires, in: *Matériaux 2006*, Dijon, 13–17 November 2006.
- [52] T. Kanit, F. N'Guyen, S. Forest, D. Jeulin, M. Reed, S. Singleton, Apparent and effective physical properties of heterogeneous materials: Representativity of samples of two materials from food industry, *Computer Methods in Applied Mechanics and Engineering* 195 (2006) 3960–3982.
- [53] K. Madi, S. Forest, D. Jeulin, M. Boussuge, Estimating RVE sizes for 2D/3D viscoplastic composite materials, in: *Matériaux 2006*, Dijon, 13–17 November 2006, hal-00144481, version 1.